

Electronic Specific Heat of $\text{La}_{2-x}\text{Sr}_x\text{CuO}_4$: Pseudogap Formation and Reduction of the Superconducting Condensation Energy

Toshiaki MATSUZAKI, Naoki MOMONO, Migaku ODA, and Masayuki IDO

Department of Physics, Hokkaido University, Sapporo 060-0810, Japan

To examine the so-called small pseudogap and the superconducting (SC) condensation energy $U(0)$, the electronic specific heat C_{el} was measured on $\text{La}_{2-x}\text{Sr}_x\text{CuO}_4$ up to ~ 120 K. In samples with doping level $p(=x)$ less than ~ 0.2 , small pseudogap behavior appears in the γ ($= C_{el}/T$) vs. T curve around the mean-field critical temperature for a d -wave superconductor T_{co} ($= 2\Delta_0/(4 \sim 5)k_B$), where Δ_0 is the maximum gap at $T \ll T_c$. The condensation energy $U(0)$ is largely reduced in the pseudogap regime ($p \lesssim 0.2$). The reduction of $U(0)$ can be well reproduced by introducing an effective SC energy scale $\Delta_0^{\text{eff}} = \beta p \Delta_0$ ($\beta = 4.5$) instead of Δ_0 . The effective SC energy scale is discussed in relation to the coherent pairing gap formed over the nodal Fermi arc.

KEYWORDS: electronic specific heat, superconducting condensation energy, pseudogap, $\text{La}_{2-x}\text{Sr}_x\text{CuO}_4$

1. Introduction

Loram *et al.* revealed that the superconducting (SC) condensation energy $U(0)$ of high- T_c cuprates was exceedingly suppressed even in a slightly underdoped region, where T_c was still high enough.¹⁻³ To clarify the origin of the exceeding reduction of $U(0)$ is expected to give an important clue to understanding the mechanism of high- T_c superconductivity, because the condensation energy $U(0)$ reflects features of the pairing mechanism and/or the collective motion of pairs. Thus this problem has been discussed from various points of view.¹⁻⁶ Loram *et al.* have argued the exceeding reduction of $U(0)$ in terms of the existence of a T -independent energy gap at the Fermi level E_F , which is persistent up to a slight overdoping level.¹⁻³ Another explanation has been proposed by Demler and Zhang on the basis of a spin-triplet particle-particle resonance, which lowers the antiferromagnetic (AFM) exchange energy in the d -wave SC state through the formation of the so-called π -resonance in the dynamic spin susceptibility $\chi(q, \omega)$.^{4,7} In this scenario, the SC condensation energy $U(0)$ comes from the difference of AFM exchange energy between the normal and superconducting states, and so $U(0)$ will be reduced greatly in samples with small doping levels whose AFM correlation is already enhanced to a large extent in the normal state. Other kind of explanation is that in the underdoped region the superconductivity will be driven by a small gain in kinetic energy caused by interplane phase coherence, which naturally leads to a small $U(0)$.⁵ Recently Lee and Salk have claimed that unusual doping-level (p) dependence of $U(0)$ can be explained within the framework of the boson-pair condensation in the SU(2) slave-boson model.⁶

Very recently it was demonstrated for $\text{La}_{2-x}\text{Sr}_x\text{CuO}_4$ (La214) that the exceeding reduction of $U(0)$ can be reproduced quantitatively by adopting the SC energy scale $\beta p \Delta_0$ ($\beta = 4.5$) instead of Δ_0 , where Δ_0 is the maximum value of the d -wave energy gap.⁸ The SC energy

scale $\beta p \Delta_0$ ($\beta = 4.5$), deduced from the phenomenological relation $T_c \sim \kappa p \Delta_0$ ($\kappa \sim 1.7$),⁹ becomes much smaller than Δ_0 at small doping levels through the factor βp , and $U(0)$ will be markedly suppressed there. On the other hand, the energy scale $\beta p \Delta_0$ ($\beta = 4.5$) becomes comparable with Δ_0 around $p(=x) = 0.22$, where no pseudogap behavior appears and the SC properties are of the BCS type. This leads naturally to the speculation that the change of the SC energy scale from Δ_0 to $\beta p \Delta_0$ will result from the development of a pseudogap in the normal state.

In many high- T_c cuprates, two types of pseudogaps appear in the normal state for $x \lesssim 0.2$; one is the so-called large pseudogap brought by the downward shift of flat bands from E_F near $(\pi, 0)$ and $(0, \pi)$, and the other is the so-called small pseudogap characterized by an energy scale of the order of Δ_0 .¹⁰⁻¹⁶ The small pseudogap was first reported as the spin gap in NMR relaxation time T_1 measurements on $\text{YBa}_2\text{Cu}_3\text{O}_{6+\delta}$,¹⁷ and has been found in many high- T_c cuprates although it was as late as last year that the spin gap was reported in inelastic neutron scattering and NMR- T_1 measurements on La214.^{18,19} Angle-resolved photoemission spectroscopy (ARPES) measurements on $\text{Bi}_2\text{Sr}_2\text{CaCu}_2\text{O}_{8+\delta}$ (Bi2212) have clarified that the small pseudogap starts to open at the Fermi surface near $(\pi, 0)$ and $(0, \pi)$ at temperature $T^*(> T_c)$. The small pseudogap grows towards the d -wave nodal points near $(\pi/2, \pi/2)$ at $T_c < T < T^*$, leaving the so-called nodal Fermi arc centered at the nodal points.²⁰ Very recently Yoshida *et al.* and Zhou *et al.* reported the existence of the nodal Fermi arc in underdoped samples of La214.^{21,22} Tunneling spectroscopy measurements on Bi2212 have demonstrated that the small pseudogap behavior becomes evident gradually around the mean-field critical temperature $T_{co} = 2\Delta_0/(4 \sim 5)k_B$ for a d -wave superconductor.²³

In the present study, the electronic specific heat C_{el} for La214 was systematically measured over a wide doping-level (p) range to examine the pseudogap formation, the

marked reduction of $U(0)$ and the interrelation between them in detail. The small pseudogap behavior appears around the temperature T' ($\sim T_{co}$) which roughly correlates with the onset temperature of the enhanced Nernst signal reported by Wang *et al.*²⁴ It was reconfirmed that the reduction of $U(0)$ becomes more conspicuous in samples with higher T' and can be well explained by the SC energy scale $\beta p \Delta_0$ ($\beta = 4.5$) over a wide p range. The SC energy scale is discussed in relation to the shrinkage of the coherent part of the pairing gap in the pseudogap regime.

2. Experimental

Ceramic samples of La214 used for the present study were prepared by using a solid reaction in an oxygen atmosphere. The SC critical temperature T_c was determined from the SC diamagnetism measured with a SQUID magnetometer. Specific heat measurements were carried out using a conventional pulsed-heat technique.

The electronic specific heat C_{el} of SC samples was obtained by subtracting the phonon term C_{ph} of an impurity-doped nonsuperconducting sample from the observed total specific heat C_{total} ; $C_{el} = C_{total} - C_{ph}$. The phonon term C_{ph} of the nonsuperconducting sample was obtained as follows. First we determined the coefficient of the T linear term of C_{el} , γ , using a C_{el}/T vs. T^2 plot at low temperatures where C_{ph} shows T^3 dependence.²⁵ Next we extracted C_{ph} by subtracting the electronic term γT from C_{total} on the assumption that γ was independent of T . We tried to use Zn impurity at first to suppress the superconductivity in the process of obtaining C_{ph} , because the Zn ion has the mass closest to that of Cu^{2+} and carries no local magnetic moment. However, since the Zn impurity modifies the phonon properties, the phonon term C_{ph}^{Zn} of the Zn-doped non-superconducting sample becomes appreciably different from the C_{ph} of the SC sample, as will be described in the following section. Then we used the phonon term C_{ph}^{Ni} obtained for an Ni-doped non-superconducting sample, although the Ni impurity carries local magnetic moment. It has been revealed that a small amount of Ni impurity removed the superconductivity and the small pseudogap behavior.²⁶

3. Results and Discussion

3.1 Electronic Specific Heat C_{el} of $La_{2-x}Sr_xCuO_4$

In Fig. 1, typical temperature dependences of C_{el} , obtained by using the phonon terms C_{ph}^{Ni} and C_{ph}^{Zn} , are shown with a C_{el}/T ($= \gamma$) vs. T plot. The $\gamma - T$ plot for C_{ph}^{Zn} shows a seeming anomaly around 15 K, and is severely distorted over the temperature range examined. On the other hand, the $\gamma - T$ plot for C_{ph}^{Ni} shows no anomaly around 15 K, and shows a plausible T -dependence of γ below and above T_c . These results imply that Zn impurity will seriously change the phonon term C_{ph} whereas the influence of Ni is very small. It has also been reported for La214 that the Zn- and Ni-impurity effects on the structural phase transition from the tetragonal phase to the orthorhombic one at temperature T_d ($\gg T_c$) are contrasting with each; T_d is little influenced by doping with Ni whereas it is enhanced appreciably by doping with Zn.²⁷ These facts mean that the nature of the phonon

system is largely modified by doping with Zn.

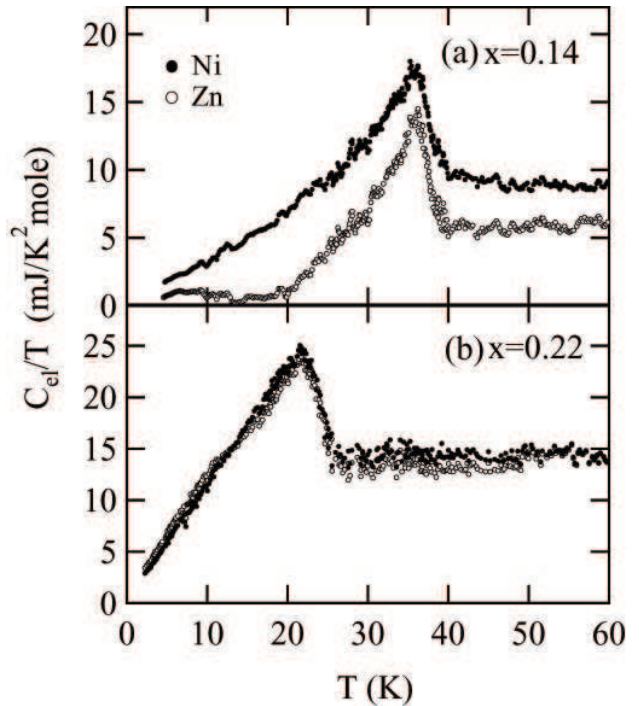


Fig. 1. T -dependence of the electronic specific heat C_{el} (C_{el}/T vs. T plot) obtained for $La_{2-x}Sr_xCuO_4$ with $x = 0.14$ and 0.22 by using different phonon terms C_{ph}^{Zn} (○) and C_{ph}^{Ni} (●).

In high T_c cuprates, it has been clarified that Zn impurity with no $3d$ -spin disturbs the AFM Cu - $3d$ -spin correlation around Zn more seriously than Ni-impurity with $3d$ -spin.²⁸⁻³¹ Since the AFM $3d$ -spin correlation couples with B_{2u} phonon modes, as has been reported in neutron scattering experiments on high- T_c cuprates,³² we can conjecture that the nature of the phonon system will be significantly modified by the serious disturbance of $3d$ -spin correlation caused by doping with Zn. This conjecture is consistent with the fact that the Zn-impurity effect on C_{ph} becomes less evident in the highly-doped $x = 0.22$ sample, where the AFM spin correlation is weakened to a large extent, as seen in Fig. 1.

3.2 Superconducting Anomaly and Pseudogap Behavior in C_{el}

Figure 2 shows the p dependence of C_{el} , obtained by subtracting the phonon term C_{ph}^{Ni} from C_{total} , with a C_{el}/T ($= \gamma$) vs. T plot. The SC anomaly appears clearly in the γ vs. T plot for all samples investigated. The anomaly for $x = 0.22$ is very similar, in both shape and size, to the BCS result for a d -wave superconductor over a wide T range except just below and above T_c , where the SC critical fluctuation effects become evident. On the other hand, the anomaly for $x < 0.2$ becomes rather different from the BCS result; namely, the γ value reaches the peak value at $T \cong T_c$ and tends to decrease more rapidly at $T < T_c$. In particular, the γ value for $x \leq 0.1$ decreases very steeply at $T < T_c$, leaving a sharp peak at T_c . The rapid decrease of γ at $T < T_c$ implies that the en-

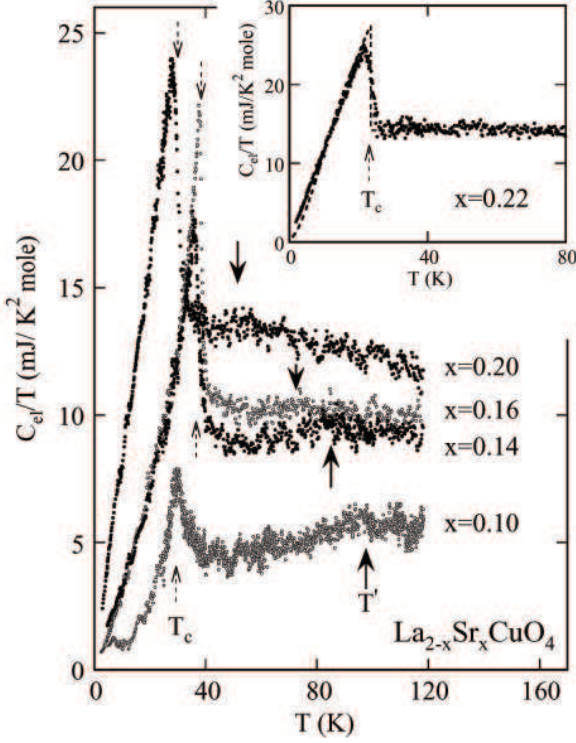


Fig. 2. Electronic specific heat C_{e1} for $\text{La}_{2-x}\text{Sr}_x\text{CuO}_4$ ($0.1 \leq x \leq 0.2$) plotted with C_{e1}/T vs. T . The inset shows the C_{e1}/T vs. T curve for $x = 0.22$. The dotted line in the inset represents the theoretical result for a d -wave BCS superconductor.

ergy gap is developed to a large extent just below T_c , as observed in tunneling spectroscopy measurements,^{15,33} and quasiparticle excitations are rather suppressed even in the neighborhood of T_c . On the other hand, the γ value tends to be enhanced at temperatures just above T_c , in particular, in samples with small doping levels. Some inhomogeneity effect, leading to the distribution of T_c , could cause the enhancement of γ at $T > T_c$. In this case, the peak anomaly at T_c would be rounded owing to the distribution of T_c . However, this is not the present case, because the peak anomaly at T_c is very sharp even in $x = 0.08$ and 0.1 samples whose γ enhancement at $T > T_c$ is most evident among samples examined. This fact means that the enhancement of γ at $T > T_c$ is not due to an inhomogeneous effect but due to the strong SC critical fluctuation effect.

It should be noted here that the γ - T curve for $x \lesssim 0.20$ shows a small, broad bump at a certain temperature T' ($> T_c$) in the normal state, and the γ value gradually decreases at $T < T'$. The temperature T' increases with lowering p ($= x$), and the decrease of γ at $T < T'$ becomes evident. The decrease of γ at $T < T'$ implies that a small pseudogap around the Fermi energy E_F will start to evolve around T' and suppress the density of states (DOS) at E_F , $N(0)$. As has been reported, T' is in agreement with the mean-field critical temperature $T_{co} \sim 2\Delta_0/4.3k_B$ (Fig. 3),³⁴⁻³⁶ where the maximum gap Δ_0 was measured in tunneling spectroscopy experiments on La214.^{23,37,38} The in-plane resistivity and the uniform susceptibility of La214 also show small anomalies

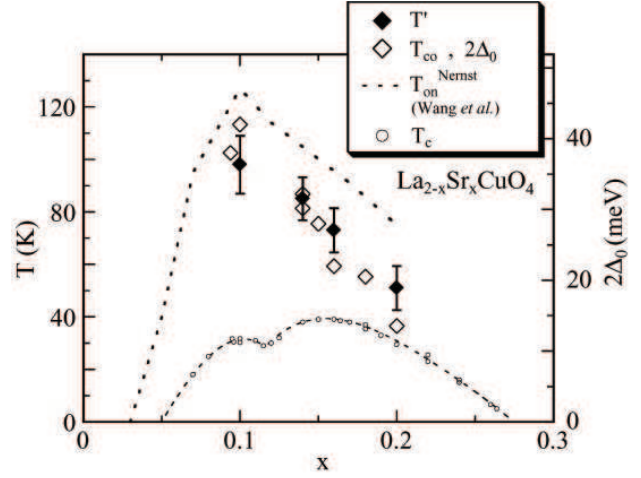


Fig. 3. Doping-level dependence of T' , T_{co} , $2\Delta_0$ and T_c . Onset temperature of the enhanced Nernst signal (T_{on}^{Nernst}) is also shown by the dotted line.²⁴ Note that for the open rhombus the left and right axes provide the scales of T_{co} and $2\Delta_0$, respectively.

around T_{co} ($\sim T'$), as in Bi2212.²³

Recently, it was reported for La214 and $\text{Bi}_2\text{Sr}_{2-y}\text{La}_y\text{CuO}_6$ that the Nernst signal enhanced by vortices or vortex-like excitations extends to temperatures well above T_c .²⁴ The anomalous Nernst signal has been interpreted in terms of strong fluctuations between the pseudogap state and d -wave SC condensates. It is worthwhile to point out the fact that both the small, broad bump in the γ - T curve and the enhanced Nernst signal appear in La214 samples for $x \lesssim 0.2$, and the temperature T' ($\sim T_{co}$) exhibiting the bump in the γ - T curve roughly correlates with the onset temperature of the enhanced Nernst signal T_{on}^{Nernst} , as shown in Fig. 3. Such a correlation between T' and T_{on}^{Nernst} confirms that the anomalous Nernst signal will be intimately related to the development of the small pseudogap in the normal state.

3.3 Superconducting Condensation Energy of $\text{La}_{2-x}\text{Sr}_x\text{CuO}_4$

The SC condensation energy $U(0)$ can be evaluated by integrating the entropy difference $S_n - S_s$ between $T = 0$ and T_c

$$U(0) = \int_0^{T_c} (S_n - S_s) dT, \quad (1)$$

where the subscripts s and n stand for the SC and hypothetical normal states at $T < T_c$, respectively. Given both γ_s and γ_n as a function of T , we can obtain the entropy S_s and S_n by executing the integration

$$S_{s,n}(T) = \int_0^T \gamma_{s,n} dT,$$

and evaluate the condensation energy $U(0)$ using eq. (1). In the present system, the SC critical fluctuation effect is so strong that we have to take the upper limit of the integration of eq. (1) to be T_{sf} ($> T_c$), instead of T_c , where γ_n ($T > T_c$) begins to increase on account of the SC critical fluctuation effect.

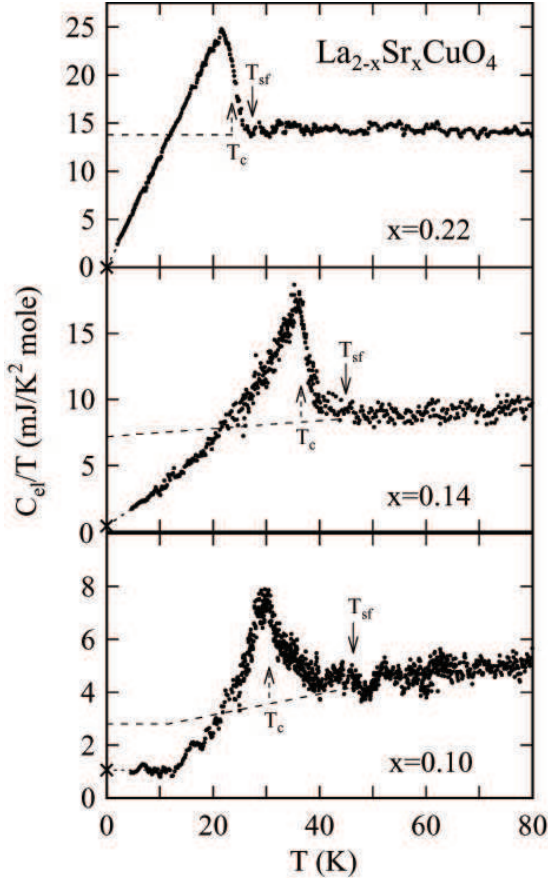


Fig. 4. T -dependence of C_{el}/T ($= \gamma$) in the superconducting state, $\gamma_s(T)$, and the normal state, $\gamma_n(T)$, for $\text{La}_{2-x}\text{Sr}_x\text{CuO}_4$. The broken line represents the hypothetical normal state value $\gamma_n(T)$ at $T < T_c$. The residual γ -value at $T = 0$ (γ_0) in the superconducting state, which was estimated in C_{el}/T vs. T^2 plots at low temperatures, is also shown on the vertical axis (\times).

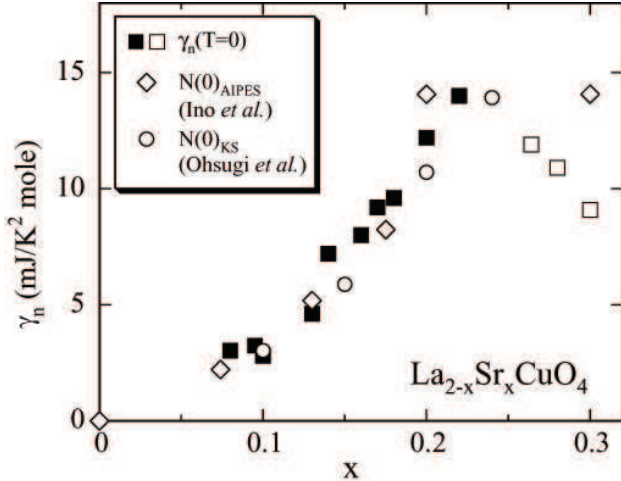


Fig. 5. Doping-level dependence of $\gamma_n(0)$ for $\text{La}_{2-x}\text{Sr}_x\text{CuO}_4$. The $\gamma_n(0)$ for non-superconducting samples with $x > 0.26$ were obtained from the conventional C/T vs. T^2 plots. The open rhombus represents the density of states at E_F , $N(0)_{\text{AIPES}}$, reported for angle-integrated photoemission spectroscopy measurements on $\text{La}_{2-x}\text{Sr}_x\text{CuO}_4$.¹⁰ The open circle represents $N(0)_{\text{KS}}$ estimated from the drop of the Knight shift below T_c .^{39,40} The $N(0)_{\text{AIPES}}$ and $N(0)_{\text{KS}}$ are normalized with $\gamma_n(0)$ at $x \approx 0.22$.

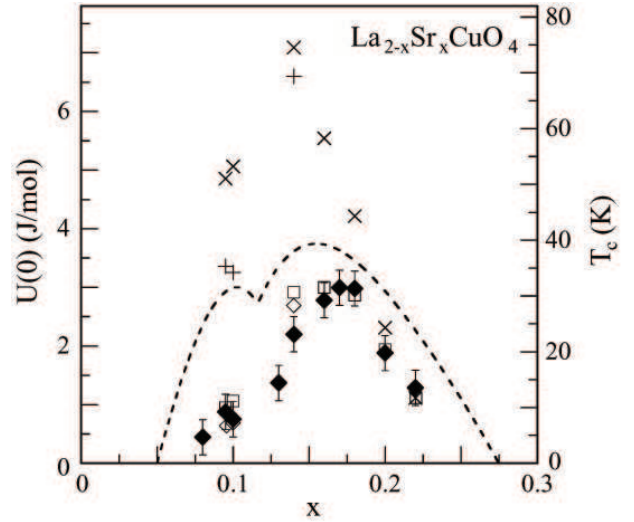


Fig. 6. Superconducting condensation energy $U(0)$ for $\text{La}_{2-x}\text{Sr}_x\text{CuO}_4$. Experimental data (\blacklozenge) obtained by executing the integral of eq. (1) are shown, together with the calculated values (\times) given by eq. (2) for the experimental values of $\gamma_n(0)$ and Δ_0 . The $U(0)$ (\square) calculated by substituting $\Delta_0^{\text{eff}} (= \beta p \Delta_0)$ for Δ_0 in eq. (2) are also shown. The condensation energy $U(0)$ was also calculated for $\Delta_0(+)$ and $\Delta_0^{\text{eff}}(\diamond)$ using $\gamma'_n = \gamma_n(0) - \gamma_0$ instead of $\gamma_n(0)$. The dotted line shows the p dependence of T_c .

In the present study, to determine the T dependence of γ_n for the hypothetical normal state, we extrapolated the data of γ_n measured at $T > T_{sf}$ down to below T_{sf} , as shown in Fig. 4. In the highly-doped $x = 0.22$ sample, since γ_n is almost constant at $T > T_{sf}$, we can safely extrapolate the data down to $T = 0$. The hypothetical normal value $\gamma_n(T < T_{sf})$ thus obtained satisfies the constraint on the second order phase transition; namely, $S_n(T_{sf}) = S_s(T_{sf})$. This constraint is often called “the entropy balance”, because excess and deficit areas of the γ_s vs. T curve, compared with γ_n ($T < T_{sf}$), must be equal with each other to satisfy the condition $S_n(T_{sf}) = S_s(T_{sf})$. On the other hand, the γ_n -value for $x \lesssim 0.2$ becomes temperature dependent at $T > T_{sf}$ on account of the small pseudogap formation, so we extrapolated the data of $\gamma_n(T > T_{sf})$ down to below T_{sf} using a declining straight line to satisfy the entropy balance (Fig. 4). Furthermore, in samples for $x \leq 0.1$, we took γ_n ($T < T_{sf}$) to be constant at $T < 0.3T_c$ because γ_s tends to be saturated at $T < 0.3T_c$ in these samples. In Fig. 5, the extrapolated value of γ_n ($T < T_{sf}$) at $T = 0$, $\gamma_n(0)$, is shown against p ($= x$). The p dependence of $\gamma_n(0)$ is in agreement with that of $N(0)$ reported in photoemission spectroscopy measurements on La214 performed by Ino *et al.*¹⁰ We can also obtain the information about $N(0)$ from the T dependence of the NMR Knight shift at $T \lesssim T_c$, because the Knight shift drops below T_c when the Fermi surface is removed by the formation of the spin-singlet pairing gap. The p dependence of $N(0)$, obtained from the data of the Cu NMR Knight shift reported by Ohsugi *et al.* for La214,^{39,40} also agrees with that of $\gamma_n(0)$, as shown in Fig. 5. The agreement between $\gamma_n(0)$ and $N(0)$ gives validity for the present extrapolat-

ing process of γ_n ($T > T_{sf}$) down to below T_{sf} . Thus we calculated the condensation energy $U(0)$ using the data of $\gamma_s(T)$ and the extrapolated γ_n ($T < T_{sf}$), and plotted the result against x in Fig. 6.

As seen in Fig. 5, $\gamma_n(0)$, namely $N(0)$, decreases rapidly at $x \lesssim 0.2$. The decreases of $N(0)$ at $x \lesssim 0.2$ result, in large part, from the downward shift of the flat band from E_F near $(p_m\pi, 0)$ and $(0, p_m\pi)$, i.e. the large pseudogap, as was demonstrated by ARPES measurements on La214.¹¹ The flat band, one of the striking features of the electronic structure in high- T_c cuprates, makes a large contribution to DOS, and so the downward shift of the flat band from E_F leads to a large reduction of $N(0)$. Furthermore, since the small pseudogap as well as the large pseudogap grows in La214 samples for $x \lesssim 0.2$,⁸ as mentioned above, the development of the small pseudogap at $T < T'$ ($\sim T_{co}$) also contributes to the reduction of $N(0)$, i.e., $\gamma_n(0)$ for $x \lesssim 0.2$.

The SC condensation energy $U(0)$ can be given approximately by

$$U(0) \approx \frac{\alpha}{2} N(0) \Delta_0^2 \approx \frac{2.1 \times 10^{-5}}{2} \alpha \gamma_n(0) \Delta_0^2 [\text{eV}] \quad (2)$$

for a d -wave superconductor ($\alpha \simeq 0.4$) with a nearly flat DOS.⁴¹ The expression can be expected to hold good in any reasonable models for the d -wave superconductivity.⁴² We calculated the condensation energy $U(0)$ using eq. (2) for $\gamma_n(0)$ (J/K²mole) (Fig. 5) and Δ_0 (eV) determined in tunneling experiments on La214 (Fig. 3).^{23,37,38} For the $x = 0.22$ sample, whose SC anomaly of C_{el} is of typical BCS type (the inset of Fig. 2), Δ_0 was estimated from T_c using the BCS relation $2\Delta_0 = 4.3k_B T_c$ for d -wave superconductors.³⁵ In the present study, since the value of γ_s at $T = 0$, estimated from the C_{el}/T vs. T^2 plot, shows a small residual value (γ_o) for $x \lesssim 0.14$, we calculated the condensation energy $U(0)$ for both $\gamma_n(0)$ and $\gamma'_n = \gamma_n(0) - \gamma_o$. The condensation energy $U(0)$ thus calculated is in good agreement with the experimental result for the overdoped $x = 0.22$ sample, as seen in Fig. 6. On the other hand, the calculated value for $x \lesssim 0.2$ is quite different from the experimental result.

The serious disagreement between experimental and calculated values of $U(0)$ at $x \lesssim 0.20$ seems to result from the modification of the nature of the pairing gap caused by the pseudogap formation. In fact, it has been pointed out that T_c roughly scales with $\kappa p \Delta_0$ ($\kappa \sim 1.7$), instead of Δ_0 , over a wide p range in the pseudogap regime,^{9,23} although a d -wave gap is completed over the entire original Fermi surface at $T \ll T_c$, with the maximum value Δ_0 at antinodal points near $(\pi, 0)$ and $(0, \pi)$. This indicates that the SC energy scale determining T_c will be proportional to $p\Delta_0$ in the pseudogap regime; namely, $k_B T_c \propto p\Delta_0$. The relation $k_B T_c \sim p\Delta_0$ was phenomenologically predicted first by Lee and Wen for the underdoped spin-gap (small pseudogap) regime although they took Δ_0 to be almost independent of p there, and then discussed microscopically on the basis of the SU(2) slave-boson model.^{43,44} Recently Tesanovic has also discussed the relation in terms of vortex-antivortex pairs.⁴⁵ Thus we recalculated $U(0)$ by substituting the SC energy scale $\beta p \Delta_0$ ($\beta = 4.5$) for Δ_0 in eq. (2), and plot the calculated

result in Fig. 6. The newly calculated values reproduce the experimental result of $U(0)$ very well over the whole p -range examined.

The new SC energy scale $\beta p \Delta_0$ ($\beta = 4.5$), introduced in the above analysis for $U(0)$, becomes smaller than Δ_0 at doping levels for the pseudogap regime ($p \lesssim 0.2$). However, it returns back to Δ_0 around the doping level $p(=x)=0.22$, where no pseudogap behavior appears and the SC properties are of the BCS type. Furthermore if we represent the SC energy scale $\beta p \Delta_0$ ($\beta = 4.5$) as Δ_0^{eff} , the phenomenological relation $k_B T_c \sim \kappa p \Delta_0$ ($\kappa \sim 1.7$) can be rewritten as $2\Delta_0^{\text{eff}} \sim 5.3k_B T_c$, which is similar to the BCS result for a d -wave superconductor. These results suggest that $\Delta_0^{\text{eff}} = \beta p \Delta_0$ ($\beta = 4.5$) may correspond to the maximum value of the effective SC gap in the pseudogap regime. In subsection 3.5, Δ_0^{eff} will be discussed in terms of the shrinkage of the coherent part of the pairing gap.

3.4 Comparison of $U(0)$ between La214 and Other Systems

Here we compare the present data of $U(0)$ with those reported by Loram's group on $Y_{0.8}Ca_{0.2}Ba_2Cu_3O_{6+\delta}$ (Y123(Ca)) and Bi2212.¹⁻³ Loram's group estimated the condensation energy $U(0)$ on the assumption that the hypothetical normal value of γ_n , $\gamma_n(T < T_{sf})$, is strongly T -dependent in samples for $p \lesssim 0.19$ and reduced to zero at $T = 0$.¹⁻³ This is because the T dependence of γ_n in the normal state ($T > T_c$) could be reproduced by assuming the existence of a T -independent gap structure near E_F which would reduce γ_n to be 0 at $T = 0$. However, since the existence of such a gap structure has not been clarified yet experimentally,^{15,33} we presumed a simple T -dependence for γ_n ($T < T_c$) with a finite value at $T = 0$, as mentioned in subsection 3.3. This discrepancy in the T dependence of γ_n ($T < T_c$) may prevent us from comparing the present data with those of the Loram group. However, we can confirm phenomenologically that $U(0)$ is almost independent of the T -dependence of γ_n ($T < T_c$) as long as the entropy balance holds between T dependences of γ_n and γ_s at $T \leq T_{sf}$. This allows us to make a comparison between the present data of $U(0)$ and the Loram group's, because the entropy balance is satisfied in both groups' analyses.

In Fig. 7, both $U(0)/U_m(0)$ and T_c/T_c^{max} , normalized with the maximum values of

$U(0)$ and T_c respectively, are shown for La214 and Bi2212 as a function of p/p_m , where p_m is the doping level at which $U(0)$ takes the maximal value $U_m(0)$. On the other hand, the original data of $U(0)$ and T_c for Y123 (Ca) are plotted against oxygen content δ , instead of p , which has one-to-one correspondence with p . In Fig. 7, we convert δ into p so that both peaks of $U(0)/U_m(0)$ vs. δ and T_c/T_c^{max} vs. δ curves for Y123(Ca) should agree with the corresponding peaks for La214, respectively. The T_c/T_c^{max} vs. p/p_m curves thus obtained for Y123(Ca) and Bi2212 are in agreement with that for La214 over a wide p range except around $p = 1/8$ in La214 and the Ortho-I ($T_c \sim 60\text{K}$) phase in Y123 where T_c becomes less dependent on $p(\delta)$. The values of $U(0)/U_m(0)$ for Y123(Ca) and Bi2212 show p dependences similar to that

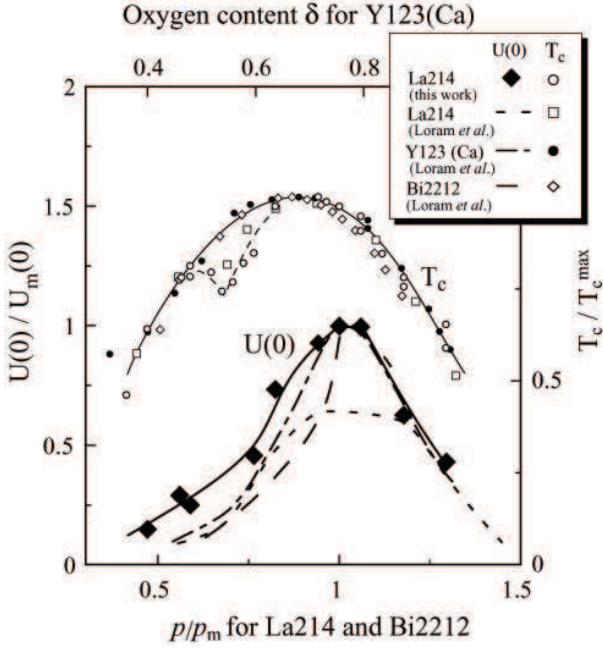


Fig. 7. Doping-level dependence of $U(0)$ for La214, $Y_{0.8}Ca_{0.2}Ba_2Cu_3O_{6+\delta}$ (Y123(Ca)), $Bi_2Sr_2CaCu_2O_{8+\delta}$ (Bi2212), plotted together with T_c . The $U(0)$ for Y123(Ca) and Bi2212 reported by Loram *et al.* are shown by the dashed dotted line and dashed line, respectively.^{1–3} $U(0)$ and T_c are normalized with their maximum values $U_m(0)$ and T_c^{\max} . The doping level p and oxygen content δ are normalized with p_m and δ_m where $U(0)$ takes the maximal value $U_m(0)$. The $U(0)$ for La214 reported by Loram *et al.* is also plotted with the same reduced scale (dotted line).¹

for La214, though $U(0)/U_m(0)$ tends to decrease faster at $p < p_m$ in Y123(Ca) and Bi2212 than in La214. The similarity in both $U(0)/U_m(0)$ vs. p/p_m and T_c/T_c^{\max} vs. p/p_m curves among La214, Y123(Ca) and Bi2212 implies that there exists no essential difference in the SC transition mechanism among them, though T_c varies from system to system.

The condensation energy $U(0)$ reported by Loram's group for La214 is also plotted in Fig. 7, where p is normalized so that the T_c vs. p curves coincide with each other.¹ The overall p ($= x$) dependence of $U(0)$ is qualitatively consistent, but the Loram data are smaller in the pseudogap regime ($x \lesssim 0.2$) than the present data. The difference of $U(0)$ can be attributed to the difference between the raw data of C_{el} measured by Loram's group and ours, because both groups adopted different ways to estimate the phonon part C_{ph} . One of the differences is that Loram's group adopted Zn impurity to destroy the superconductivity in the standard sample on the overdoped sample, whereas Ni impurity was used in the present study.

3.5 Coherent Pairing Gap

In high- T_c cuprates with low doping levels, the nodal parts of the Fermi line near $(\pi/2, \pi/2)$ dominate the in-plane transport; i.e., in-plane mobility of carriers on the nodal parts of the Fermi surface is much higher than on the antinodal parts near $(\pi, 0)$ and $(0, \pi)$.^{46–48} This is typically demonstrated by the following observation:

the Fermi surface is truncated near $(\pi, 0)$ and $(0, \pi)$ by the small pseudogap formation at $T \lesssim T_{co}$, leaving the so-called nodal Fermi arcs,²⁰ but the in-plane resistivity remains almost unchanged.⁴⁹ The pairing of mobile carriers with high in-plane mobility is expected to play a crucial role in making the collective pair motion coherent.^{46, 47} Therefore, the carriers on the nodal Fermi arcs are expected to drive the SC phase transition when they start to form pairs.^{44, 46–48, 50} This directs our attention to the possibility that in the pseudogap regime the pairing gap formed over the nodal Fermi arcs will function as the coherent pairing gap, namely, the effective SC gap which dominates T_c and $U(0)$.

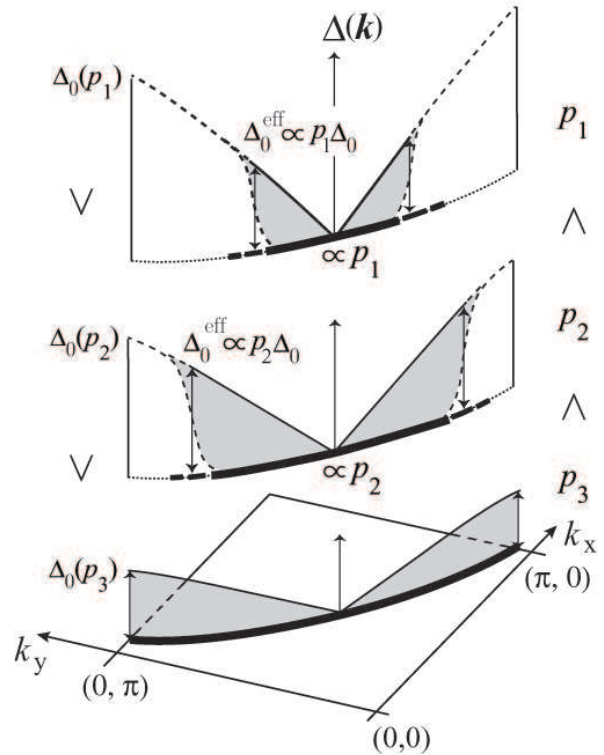


Fig. 8. Schematic illustration for doping dependence of a small pseudogap at $T \sim T_c$ (dotted line) and the nodal Fermi arc (bold solid line) in $k_x - k_y$ space. The effective SC pairing gap (gray area) is developed over the nodal Fermi arc at $T < T_c$, and the effective SC gap together with the small pseudogap completes a d -wave energy gap over the underlying Fermi line. The upper, middle and bottom figures correspond to an underdoping level (p_1), nearly optimal doping (p_2), and the overdoping (p_3) at which no pseudogap behavior appears, respectively. A line with arrow heads shows the maximum value of the effective SC gap $\Delta_0^{\text{eff}} \propto p\Delta_0$, where Δ_0 is the maximum value of the energy gap at $T < T_c$ ($\Delta_0(p_1) > g\Delta_0(p_2) > g\Delta_0(p_3)$).

The hypothetical normal state value $\gamma_n(0)$, namely $N(0)$, will give us information about the linear dimension of the Fermi arc at $T \sim T_c$, because it will be proportional to the dimension of the arc if the local DOS, $n(0)$, is constant over the Fermi line. As seen in Fig. 5, $\gamma_n(0)$ and $N(0)$ show a tendency for linear p dependence below $x \sim 0.2$, suggesting that the dimension of the nodal Fermi arc will be roughly proportional to p ($= x$) there.

Furthermore, because of the distortion of the gap function caused by the higher harmonic in high- T_c cuprates, the pairing gap at $T \ll T_c$ has a rather linear dispersion along the Fermi line in a slightly overdoped region as well as the underdoped one.⁵¹ Thus, if the dimension of the nodal Fermi arc at $T \sim T_c$ is proportional to p ($= x$), as suggested above, the gap size at the edge of the nodal arcs is roughly proportional to $p\Delta_0$, as shown schematically in Fig. 8. This gives an explanation for the maximum value of the effective SC gap $\Delta_0^{\text{eff}} = \beta p\Delta_0$ ($\beta = \text{const.}$), introduced in the present analysis for $U(0)$. Such a picture is almost the same as the scenario proposed by Wen *et al.* to explain the relation $k_B T_c \sim p\Delta_0$ microscopically on the basis of the SU(2) slave-boson model, which predicts that a hole pocket with no shadow band at $\omega = 0$ will appear near $(\pi/2, \pi/2)$, namely the nodal Fermi arc, in the spin gap regime.^{44, 52}

It is noteworthy here that the results of the electronic Raman scattering measurements on high- T_c cuprates are consistent with the present proposition that the coherent part of the pairing gap shrinks toward nodal points as the small pseudogap grows. Electronic Raman scattering measurements are expected to give more direct information about the coherent pairing gap than ARPES and tunneling spectroscopy measurements, because the electronic Raman response to superconductors is relevant to the coherence factor with even parity.⁵³ It has been reported for La214 as well as Bi2212 and Y123 that the B_{1g} Raman continua, weighing out the antinodal parts of the Fermi surface, are indicative of marked suppression of the coherent pairing gap in the underdoped region, whereas the B_{2g} continua, weighing out nodal parts, indicate the existence of the coherent pairing gap Δ_{coh} .^{53–56} Such results in Raman scattering experiments mean that the coherent pairing gap will be located near nodal points, at least, in the underdoped region, which is consistent with the present proposition. The coherent pairing gap Δ_{coh} may correspond to the effective SC gap determining T_c and $U(0)$.

The present proposition is also consistent with recent ARPES results measured by Zhou *et al.* on underdoped La214 samples; the well-defined quasiparticle peak exists on the nodal part of the Fermi line, but away from the nodal part it becomes broader and fades out rather abruptly.²²

4. Summary

The electronic specific heat C_{el} was systematically measured on $\text{La}_{2-x}\text{Sr}_x\text{CuO}_4$ (La214) to reexamine the development of the small pseudogap in the normal state ($T > T_c$) and the superconducting condensation energy at $T=0, U(0)$. The results obtained in the present study are summarized as follows.

1) The small pseudogap behavior appears in the $\gamma - T$ plot at temperature $T' \sim T_{\text{co}}$; the γ value, namely $N(0)$, shows a small bump at T' and is progressively suppressed at $T < T'$. The temperature T' ($\sim T_{\text{co}}$) roughly correlates with the onset temperature of the enhanced Nernst signal, reported by Wang *et al.* on La214.²⁴

2) We confirmed that $U(0)$ was markedly reduced in the pseudogap regime. The reduction of $U(0)$ can be

quantitatively explained by using the effective SC energy scale $\Delta_0^{\text{eff}} = \beta p\Delta_0$ ($\beta = 4.5$), instead of Δ_0 , and the DOS associated with the nodal Fermi surface which is removed by the pairing gap formation at $T < T_c$.

3) To explain the effective SC energy scale Δ_0^{eff} in the pseudogap regime, we pointed out the possibility that the pairing gap formed over the nodal Fermi arcs at $T < T_c$ will play a role as the coherent pairing gap, namely, the effective SC gap determining T_c and $U(0)$.

Acknowledgment

We would like to thank professor F. J. Ohkawa, professor S.-H. S. Salk and professor Z. Tesanovic for many stimulating discussions. This work was supported in part by Grants-in-Aid for Scientific Research on Priority Area (Novel Quantum Phenomena in Transition Metal Oxides) and on Projects (No 13440104, 15340104, 15740193) from the Ministry of Education, Culture, Science, Sports and Technology of Japan.

- 1) J. W. Laram, K. A. Mirza, W. Y. Cooper, and J. M. Wada: J. Supercon. **7**, (1994) 243.
- 2) J. W. Laram, K. A. Mirza, W. Y. Cooper, and J. L. Tallon: J. Phys. Chem. **59**, (1998) 2091.
- 3) J. W. Laram, J. L. Luo, W. Y. Cooper, and J. L. Tallon: Physica C **341-348**, (2000) 831.
- 4) E. Demler and S.-C. Zhang: Nature **396**, (1998) 733.
- 5) P. W. Anderson: Science **279**, (1998) 1196.
- 6) S. S. Lee and S.-H. S. Salk: cond-mat/0301431.
- 7) D. J. Scalapino and S. White: Phys. Rev. B **58**, (1998) 8222.
- 8) N. Momono, T. Matsuzaki, M. Oda, and M. Ido: J. Phys. Soc. Jpn. **71**, (2002) 2832.
- 9) M. Ido, N. Momono, and M. Oda: J. Low Temp. Phys. **117**, (1999) 329.
- 10) A. Ino, C. Kim, T. Mizokawa, Z.-X. Shen, A. Fujimori, M. Takaba, K. Tamasaku, H. Eisaki, and S. Uchida: Phys. Rev. Lett. **81**, (1998) 2124.
- 11) A. Ino, C. Kim, M. Nakamura, T. Yoshida, T. Mizokawa, Z.-X. Shen, A. Fujimori, T. Kakeshita, H. Eisaki, and S. Uchida: Phys. Rev. B **65**, (2002) 94504.
- 12) T. Takahashi, T. Sato, T. Yokoya, T. Kamiyama, Y. Naitoh, T. Mochiku, K. Yamada, Y. Endoh and K. Kadowaki: J. Phys. and Chem. Solids **62** (2001) 41.
- 13) A. G. Loeser, Z.-X. Shen, D. S. Dessau, D. S. Marshall, C. H. Park, P. Fournier, and K. Kapitulnik: Science **273**, (1996) 325.
- 14) J. M. Harris, Z.-X. Shen, P. J. White, D. S. Marshall, M. C. Sxhabel, J. N. Eckdtein, and I. Bozovic: Phys. Rev. B **54**, (1996) 15665.
- 15) C. Renner, B. Revaz, K. Kadowaki, I. Maggio-April, and Ø. Fischer: Phys. Rev. Lett. **80**, (1998) 3606.
- 16) T. Timusk and B. Statt: Report on Progress in Physics **62**, (1999).
- 17) H. Yasuoka, T. Imai and T. Shimizu: Springer Series in Solid State Science, **89**, Strong Correlation and Superconductivity, (Springer-Verlag, New York, 1989), p. 254.
- 18) C. H. Lee, K. Yamada, H. Hiraka, C. R. Venkateswara Rao, and Y. Endoh: Phys. Rev. B **67**, (2003) 134521.
- 19) Y. Itoh, T. Machi, N. Koshizuka, M. Murakami, H. Yamagata, and M. Matsunuma: submitted to Phys. Rev. B.
- 20) M. R. Norman, H. Ding, M. Randeria, J. C. Campuzano, T. Yokoya, T. Takeuchi, T. Takahashi, T. Mochiku, K. Kadowaki, P. Guptasarma, and D. G. Hinks: Nature **392**, (1998) 157.
- 21) T. Yoshida, X. J. Zhou, T. Sasagawa, W. L. Yang, P. V. Bogdanov, L. Lanzara, Z. Hussain, T. Mizokawa, A. Fujimori, H. Eisaki, Z.-X. Shen, T. Kakeshita, and S. Uchida, Phys. Rev. Lett. **91**, (2003) 27001.
- 22) X. J. Zhou, Phys. Rev. Lett. **92**, (2004) 187001.
- 23) T. Nakano, N. Momono, M. Oda, and M. Ido: J. Phys. Soc.

- Jpn. **67**, (1998) 2622.
- 24) Y. Wang, Z. A. Xu, T. Kakeshita, S. Uchida, S. Ono, Y. Ando, and N. P. Ong: Phys. Rev. B **64**, (2001) 224519.
- 25) N. Momono and M. Ido: Physica C **264**, (1996) 311.
- 26) T. Nagata, N. Momono, S. Takahashi, M. Oda, and M. Ido: Physica C **264-365**, (2001) 430.
- 27) N. Momono, T. Nagata, T. Matsuzaki, M. Oda, and M. Ido: New Trends in Superconductivity (Kluwer Academic Publishers, Netherlands, 2002), p. 167.
- 28) K. Ishida, Y. Kitaoka, N. Ogata, T. Kamino, K. Asayama, J. R. Cooper, and N. Athanassopoulou: J. Phys. Soc. Jpn. **62**, (1993) 2803.
- 29) T. Nakano, N. Momono, T. Nagata, M. Oda, and M. Ido: Phys. Rev. B **58**, (1998) 5831.
- 30) M.-H. Julien, T. Feher, M. Horvatic, C. Berthier, O. N. Bakharev, P. Segransan, G. Collin, and J.-F. Marucco: Phys. Rev. Lett. **84**, (2000) 3422.
- 31) N. W. Y. Itoh, T. Machi and N. Koshizuka: J. Phys. Soc. Jpn. **70**, (2001) 644.
- 32) H. Harashina, K. Kodama, S. Shamoto, M. Sato, K. Kakurai, and M. Nishi: Physica C **263**, (1996) 257.
- 33) R. M. Dipasupil, M. Oda, N. Momono, and M. Ido: J. Phys. Soc. Jpn. **71**, (2002) 1535.
- 34) F. J. Ohkawa, J. Phys. Soc. Jpn. **56**, (1987) 2267.
- 35) H. Won and K. Maki: Phys. Rev. B **49**, (1994) 1397.
- 36) T. Tanamoto, K. Khono, and H. Fukuyama: J. Phys. Soc. Jpn. **61**, (1992) 1886.
- 37) The value of Δ_0 for $x = 0.095$ was estimated from the point-contact junction tunneling spectra by M. Oda, L. Ozyuzer, J. F. Zasadzinski and K. E. Gray: which has not been published.
- 38) The maximum gap Δ_0 for $x = 0.1$ was measured by point-contact junction tunneling spectroscopy on single crystals in the present study.
- 39) S. Ohsugi, Y. Kitaoka, G.-q. K. Ishida Zheng, and K. Asayama: J. Phys. Soc. Jpn. **63**, (1994) 700.
- 40) The KS for $x = 0.24$ reported in ref. 38 has a large residual value at $T \ll T_c$, presumably, due to some inhomogeneous effect. Then we estimated $N(0)_{KS}$ for $x = 0.24$ by assuming that the KS for $x = 0.24$ would drop to a level comparable with that for other doping levels at $T \ll T_c$ if the inhomogeneous effect on the KS could be removed.
- 41) Y. Sun and K. Maki: Phys. Rev. B **51**, (1995) 6059.
- 42) P. W. Anderson, Science **268**, (1995) 1154.
- 43) P. A. Lee and X. G. Wen: Phys. Rev. Lett. **78**, (1997) 4111.
- 44) X. G. Wen and P. A. Lee: Phys. Rev. Lett. **80**, (1998) 2193.
- 45) Z. Tesanovic, private communication.
- 46) D. Pines, Physica C **282-187**, (1997) 273.
- 47) V. B. Geshkenbein, L. B. Ioffe, and A. I. Larkin: Phys. Rev. B **55**, (1997) 3173.
- 48) N. Furukawa, T. M. Rice, and M. Salmhofer: Phys. Rev. Lett. **81**, (1998) 3195.
- 49) Y. Yanase and K. Yamada: J. Phys. Soc. Jpn. **68**, (1999) 548.
- 50) C. H. A. Lauchli and T. M. Rice: Phys. Rev. Lett. **92**, (2004) 37006.
- 51) J. Mesot, M. R. Norman, H. Ding, M. Randeria, J. C. Campuzano, A. Paramakanti, H. M. Fretwell, A. Kaminski, T. Takeuchi, T. Yokoya, T. Sato, T. Takahashi, T. Mochiku, and K. Kadowaki: Phys. Rev. Lett. **83**, (1999) 840.
- 52) P. A. Lee, N. Nagaosa, T.-K. Ng, and X. G. Wen: Phys. Rev. B **57**, (1998) 6003.
- 53) M. Opel, R. Nemetschek, C. Hoffman, R. Philipp, P. F. Muller, R. Hackl, I. Tutto, W. Erb, B. Revaz, and E. Walker: Phys. Rev. B **61**, (2000) 9752.
- 54) J. G. Naeini, X. K. Chen, J. C. Irwin, M. Okuya, T. Kimura, and K. Kishio: Phys. Rev. B **59**, (1999) 9642.
- 55) G. Deutscher, Nature **397**, (1999) 410.
- 56) N. Momono, R. M. Dipasupil, S. Manda, T. Nagata, M. Oda, M. Ido, and A. Sakai: Physica C **341**, (2000) 909.